Low-Dose Fractionated Irradiation Selectivly Regulate CSPGs and PNNs, Promote Serotonergic Axonal Regeneration

Qiang Zhang (zhangqiang_glia@126.com)
Tongji Hospital of Tongji Medical College of Huazhong University of Science and Technology
https://orcid.org/0000-0002-3680-6394

Jiao Xu
Tongji Hospital of Tongji Medical College of Huazhong University of Science and Technology

Xiaoxiao Xiong
Tongji Hospital of Tongji Medical College of Huazhong University of Science and Technology

Bifeng Zhu
Tongji Hospital of Tongji Medical College of Huazhong University of Science and Technology

Bo Zhu
Tongji Hospital of Tongji Medical College of Huazhong University of Science and Technology

Ying Xiong
Tongji Hospital of Tongji Medical College of Huazhong University of Science and Technology
https://orcid.org/0000-0002-6270-5220

Wei Wang
Tongji Hospital of Tongji Medical College of Huazhong University of Science and Technology

Research Article

Keywords: CS-A, CS-C, PNNs, 5-hydroxytryptamine, low-dose fractionated therapy, axonal regeneration

Posted Date: July 9th, 2021

DOI: https://doi.org/10.21203/rs.3.rs-514017/v1

Abstract

Chondroitin sulphate proteoglycans (CSPGs) are major components to impeding axonal regeneration, condense in the extracellular-matrix to form perineuronal nets (PNNs) which interdigitate with axonal contacts. Each CSPG comprises a core protein with covalently attached chondroitin-sulfate glycosaminoglycan side chains (CS moieties). In the past, the representative treatment for CSPGs were chondroitinase-ABC which destroys all CS moieties. However, recent rodents researches found some CS moieties promote axon regeneration rather than inhibit axon regeneration. Using a canine model of spinal cord injury (SCI), which is a superior translational model for progressing rodent data into clinical practice, we showed that specific sulfation patterns of CS moieties play different role in modulation of axon re-growth. Upregulated CS-A expression occurred at 1-day post-SCI, earlier than CS-C expression which was increased at 14-days post-SCI. CS-A was mainly colocalized with astrocytes but CS-C was upregulated in both astrocytes and neurons/axons. Treatment with low-dose fractionated irradiation (LDI) significantly inhibited the expressions of astrocyte-associated CS-A and CS-A-enriched PNNs, but no inhibitory effect on CS-C and CS-C-enriched PNNs. There was a positive correlation between a reduction of CS-A-enriched PNNs and an increase of serotonergic (5-hydroxytryptamine, 5-HT) axonal sprouting. Increased serotonergic axon sprouting proximal to the lesion accompanied 5HT receptor up regulation following LDI treatment. Furthermore, LDI treatment promoted hindlimb motor function recovery following SCI. Taken together, our findings show that specific sulfation patterns of CS moieties and CSPG-enriched PNNs involved in carrying instructions for regulating axonal regeneration and that LDI treatment may be an efficacious strategy for treating SCI.

Introduction

Spinal cord injury (SCI) causes severe sensorimotor dysfunctions, which induces long-term life difficulties in affected individuals. Axonal regeneration and re-innervation have emerged as important mechanisms underlying functional recovery processes following SCI (Tohda and Kuboyama 2011; Fink et al. 2017; O'Shea et al. 2017). Recent evidence suggests that many repulsive cues inhibit regenerative axonal growth and lead to poor or negligible recovery of motor function (Akbik et al. 2012; Masu 2016).

Chondroitin sulphate proteoglycans (CSPGs) are amongst the key repulsive cues for axon regeneration in injured central nervous system (CNS) tissue. In the CNS, CSPGs condense around neurons soma and proximal dendrites to form perineuronal nets (PNNs), which are specialized extracellular-matrix structures that interdigitate with axonal and synaptic contacts (Ye and Miao 2013). PNNs are implicated in the termination of critical periods during development, as well in impeding axonal regeneration and synaptic plasticity in adulthood (Beurdeley et al. 2012; Sorg et al. 2016; Banerjee et al. 2017). The chondroitin-sulfate glycosaminoglycan side chains (CS moieties) of CSPGs are responsible for PNN formation and control the critical periods for plasticity of multiple circuits (Bradbury et al. 2002; Pizzorusso et al. 2002; Hou et al. 2017; Sullivan et al. 2018; Fawcett et al. 2019). The CS moieties are complex unbranched polysaccharides of variable length with a backbone structure composed of a repeating disaccharide unit consisting of D-glucuronic acid (GlcA) and N-acetyl-D-galactosamine (GalNAc) (Yutsudo and Kitagawa

2015). This simple repetitive structure can then undergo extensive modification by sulfation at the C4 or C6 position of GalNAc residues during biosynthesis. During biosynthesis, individual GalNAc residues of the repeated disaccharide units can be sulfated at C6 or C4 by chondroitin 6-O-sulfotransferase-1 (C6ST-1) and chondroitin 4-O-sulfotransferase-1 (C4ST-1), respectively (Mikami et al. 2003). Previous studies have found that changes in the activities of C6ST-1/C4ST-1 induce developmental increases/decreases in the 4-sulfation/6-sulfation ratio of CSPGs during development and in several CNS diseases (Miyata et al. 2012). However, it remains largely unknown whether changes in specific sulfation patterns regulates axonal plasticity.

Following CNS disease and injuries, high levels of CSPGs are found proximal to the lesion and form distinct PNNs (Brown et al. 2012), among which CS-A (chondroitin-4-sulfation)-enriched PNNs and CS-C (chondroitin-6-sulfation)-enriched PNNs exhibit different degrees of upregulated expression. CS-A-enriched PNNs can be labeled with Wisteria floribunda agglutinin (WFA), whereas CS-C-enriched PNNs can be labeled with a CS56 antibody (Miyata and Kitagawa 2015). Previous studies have demonstrated that elimination of CSPGs with chondroitinase ABC induces neuroprotective effects (Lee et al. 2010). However, recent axon regeneration studies, utilized rodents model, have suggested that CS moieties can act as growth factor or inhibitory molecules hinging on their sulfation status (Miyata et al. 2012; Yutsudo and Kitagawa 2015). Moreover, a recent study demonstrated that knocking out CSPGs exacerbates tissue loss, inflammation and neurologic deficits after brain injury (Schafer and Tegeder 2018). The importance of specific sulfation patterns of CS moieties to axonal regeneration might have been overlooked in previous studies because chondroitinase-ABC treatment destroys all CS moieties.

Recently, single-dose X-irradiation shown potential in the amelioration of functional deficits caused by SCI in rodents (Ridet et al., 2000; Azria et al., 2012; Kim et al., 2013; LeRoux et al., 2014). A continual administration of low-dose fractionated irradiation (LDI) treatment could show a more pronounced blocking effect on the dynamic glial reaction than the single-dose treatment. Our previous beagle dogs SCI study also showed that LDI promoted axonal regeneration through inhibiting CSPG production (Zhang et al. 2017). However, the relationship between sulfation patterns of CS moieties and axonal regeneration has still not been addressed.

The effect of LDI treatment on functional receptors of CSPGs and 5-HT receptors also need to be clarified. CSPGs work with their receptors, Nogo receptors and leukocyte common antigen-related receptor protein tyrosine phosphatases (LAR-RPTPs), initiated promoted/inhibitory effects on axonal growth and guidance (Tran et al. 2018). Interactions of CSPGs with RPTPσ or LAR have been shown in modulation of axonal regeneration and dendritic-spine formation through ADAM10 shedding, RhoA activation and tropomyosin-related kinases dephosphorylation (Kurihara and Yamashita 2012; Dyck et al. 2015; Lang et al. 2015; Fisher et al. 2011). High-affinity binding between CSPGs with NgR1/3 also has been demonstrated, knockout of *NgR1* and *NgR3* significantly promoted mice axonal regeneration following injury (Dickendesher et al. 2012). Loss of descending 5-hydroxytryptaminergic nerve fiber was involved in locomotor impairment in rodents, 5-HT receptors (including 5-HT2c/a and 5-HT7 receptors) expression are also important for locomotion recovery modulation following SCI (Slawinska et al. 2014).

Thus, we hypothesized that sulfation patterns of CS moieties are relevant to axonal regeneration because of their putative influence on the formation of specific CS-enriched PNNs. To test this hypothesis, utilized beagle dog SCI model, we examined CS moieties sulfation patterns and PNN formation proximal to the lesion. Additionally, we aimed to clarify whether or not there is a change in the expression levels of CSPG receptors following SCI and, if so, whether and which receptors affect axonal regeneration. Finally, we investigated whether the neuroprotective effects of LDI treatment are mediated via alterations of sulfation patterns that influence PNN formation. Previous studies on spinal cord injury were more based on rodent models, but, due to the anatomical, molecular and functional differences, these findings cannot be made in humans directly. CSPGs have been studied, and chondroitinase used, in several large animal models of spinal cord injury including dog, cat, and non-human primate (Tester and Howland 2008; Jefferson et al. 2011; Muir et al. 2019; Doperalski et al. 2020). Large animal may more useful for developing therapeutic strategies in humans, and canine SCI model might be considered as intermediate between rodent study and human clinical trials.

Experimental Procedures

Animals and surgery

This study was carried out in accordance with the recommendations of the National Institute of Health Guide for the Care and Use of Laboratory Animals (NIH Publications No. 80 − 23) revised 1996. The procedures were performed on the animals in accordance with protocols approved **(TJA-2019015)** by the Institutional Animal Care and Use Committee of Tongji Hospital, Tongji Medical College, Huazhong University of Science and Technology. All surgery was performed under anesthesia with pentobarbital and isoflurane, and all efforts were made to minimize the number of animals used and their suffering.

According to the principle of completely random, adult beagle dogs (n = 30, 18.5–22.0 kg) were divided into the sham-operated group **(Two time points, the number of animals at each time point = 5)**, SCI group **(Two time points, the number of animals at each time point = 5)**, LDI groups **(Two time points, the number of animals at each time point = 5)**. **The sample size was determined as our previous study, in particular, the sample size was calculated by PASS 15 (power = 0.90, alpha = 0.05, G = 3, inputted mean and SEMs and calculated the sample size).** All dogs were anesthetized with 35 mg/kg of pentobarbital, maintained with 1–2% isoflurane, as described previously (Koshman et al. 2018; Goya et al. 2018). All operations were performed by the same spine surgeon who were blinded to the study. Under aseptic conditions, the laminectomy exposed the spinal cord at T9-T10 vertebral level. In the sham-operated group, only the laminectomy was performed without any other operation. In the animals of SCI group and LDI group, a tiny incision was made, the overlying meninges were slit, one micro guide wire was placed on the longitudinal axis of the spinal cord to avoid the injury of the contralateral tissue by the scalpel, and the left hemi-cord was completely transected. Following the operation completed, the incision was immediately covered with a piece of Durafilm (American Durafilm Company Inc, USA), and gelfoam filled the tissue loss dued to the laminectomy. The overlying muscles and skin were then sutured. All these consistent operations were to avoid lesion variability within or across groups of animals.

Food and water intake of the dogs were monitored during the study. Animals recovered from surgery in a warm and comfortable room, and were returned to their quarters, penicillin were administered to prevent infection, a balanced diet including plenty of proteins was gave to the dogs, dogs' bladders were expressed 2–3 times daily until urinary incontinence disappeared. The skin also was kept clean and free of body fluids,cages were kept with very soft blankets to avoid excessive pressure and tannic acid was applied to prevent pressure ulcer.

In the LDI group, LDI program was conducted starting at 1day post-injury and continuous conducted for 14 days. No LDI was conducted in the sham-operated and SCI group. First, modified Tarlov-grading scores for locomotor function were carried at days 1, 14 and 60 post-injury, and then all dogs were euthanized with an excessive dose of barbiturates (100mg/kg) at 14-days (n = 5) and 60-days (n = 5) post-SCI, and samples of spinal cord were quickly removed on ice for further research. The samples were equally divided into two parts along the longitudinal axis of the spinal cord, half of the samples were used for morphological analysis and half for Western blot analysis.

Low-dose-fractionated irradiation therapy

Irradiation was delivered by an X-ray generator with a dose rate of 101.7 cGy/min, a hybrid orthovoltage unit operating at 250 kVp, 10 mA with 0.25 mm Cu filtration, and delivered at a distance of 50 cm from the dogs' skin. The exposure field was 30 mm ×15 mm (length × width), and the inner boundary was the spinal cord. Previous studies showed that, for human spinal cord, the clinical-tolerance-dose values are 45–50 Gy and 33 Gy when delivered in daily fractions of 2 Gy and 3 Gy, respectively (Marcus and Million 1990; Schultheiss 1990; Khan et al. 1999). In the present study, the total and fractional doses of radiotherapy were determined based on these previous studies and our previous study (Zhang et al. 2017). The LDI protocol was: LDI was performed beginning at 1-day post-SCI, and the irradiation was performed once a day for 14 days, each fractionated dose was 2 Gy, the total dose was 28 Gy across 14 fractions.

Immunohistochemistry

Briefly, samples of spinal cord were quickly removed from the vertebral column on ice, fixed with 4% paraformaldehyde overnight, washed thrice in 0.1 M PBS, immersed in 30% sucrose solution until samples sank. The optimum cutting temperature compound (Sakura, USA) then blocked the spinal cord samples. The samples were sectioned at a thickness of 40 μm on a sliding microtome (CM1900, Leica, Germany). The sections were then rinsed thrice with 0.1 M PBS, incubated with 0.2% Triton X-100 containing 1% bovine serum albumin (BSA) for 2 h, washed thrice in PBS. The sections were incubated overnight at 4°C with the primary antibodies (Table 1). Longitudinal section (cut along the longitudinal axis of the spinal cord) were stained for MAP-2/5-HT, GFAP and CSPGs specific antibodies to identify the axon regeneration mecyhanism. Sagittal sections through the lesion were stained for MAP-2 and CSPG receptors antibodies to identify the result of LDI treatment on CSPGs-CSPGs receptors binding activity. The sections were washed thrice with PBS, incubated with AffiniPure donkey anti-mouse fluorescein isothiocyanate (FITC)-conjugated secondary antibodies (1:200; Code number: 715-095-150, Jackson

ImmunoResearch), AffiniPure donkey anti-rabbit cyanine3 (Cy3)-conjugated secondary antibodies (1:200; Code number: 711-165-152, Jackson ImmunoResearch), AffiniPure donkey anti-goat cyanine3 (Cy3)-conjugated secondary antibodies (1:200; Code number: 705-165-003, Jackson ImmunoResearch), for 60 min at room temperature. Instead of the primary antibodies, nonspecific IgG was used for negative controls.

After tissue clearing, sections were imaged by a laser scanning confocal microscope (FV1000, Olympus, Japan). Images quantification was performed by two independent observers using ImageJ software. To quantify CSA/CSC and MAP-2 (+) neuron/axon density at injury site in sham-operated, SCI and LDI treatment group, CSA/CSC and MAP-2 immunoreactivities were determined by thresholding above background level. **15 slices per animal were used for quantification.** To quantify the number of MAP-2 (+) or 5-HT (+) neuron/axons, 50 μm square grids were generated over the entire image, every 6th square was quantified, only MAP-2 (+) or 5-HT (+) signal that is linear, at least 1 μm in length was identified as one axon. For quantification of positive cell percentage, cells touching the left side line and bottom line of a square were disregarded.

Western blotting

To investigate C4ST-1 protein expressions, tissue samples (20 mm length centered at the injury site) were harvested, homogenized in lysis buffer (0.1-M NaCl; 0.01-M Tris-HCl at a pH of 7.5; 1-mM EDTA; 1-mM PMSF; and 1 mg/mL of aprotinin), centrifuged at 12,000 g (15 min at 4°C). Sodium dodecyl sulfate (SDS)-polyacrylamide gel electrophoresis (PAGE) was utilized to analyze protein extracts (20–100 mg/lane). Protein was then transferred from the gel to nitrocellulose membranes after electrophoresis. The nitrocellulose membranes were blocked with 5% non-fat milk solution in TBS-0.1% Tween, incubated with anti-C4ST-1 (1:200) antibody overnight at 4°C. The anti-β-actin antibody (1:5,000, Neomarkers, CA) was blotted to confirm equal protein loading. After incubated with peroxidase-linked secondary antibody for 2 h in room temperature, C4ST-1 protein was visualized using an enhanced chemiluminescent system (Supersignal West Pico Trial Kit, 34577, Pierce, CA). **The specificity of antibodies was compared between rat spinal cord samples and canine spinal cord samples, the western blot results showed that the response of the rat and canine samples to the antibody was similar (Supplement.1).** For quantitative analysis, the protein bands intensity was analyzed by densitometry using the Molecular Analyst software.

Three-dimensional image acquisition and reconstruction

Three-dimensional image acquisition and reconstruction were performed as previously described (Zhang et al. 1999). Briefly, vibratome sections were incubated with the CS-56 antibody (1:100, Sigma-Aldrich) or Biotinylated WFA lectin (Vector laboratories, CA, USA) for three days at 4°C, and then incubated with Cy3-conjugated secondary antibodies (1:200, Jackson ImmunoResearch) or Alexa 488/594 conjugated streptavidin. These vibratome sections were then incubated with the 5-HT antibody (1:100, ImmunoStar) at 4°C for three days, and then incubated with FITC-conjugated secondary antibodies (1:200, Jackson ImmunoResearch). The sections were analyzed with an Olympus FV1500 confocal-imaging system. Microscopic data were acquired with a 40X objective lens with a numerical aperture. The red (Cy3) and

green (FITC) fluorochromes in the sections were excited by a laser beam at568 nm and 488 nm, and the emissions were acquired with two separate photomultiplier tubes through 585-nm and 522-nm emission filters, respectively. High-resolution images from the areas located in the 10X objective were acquired with 40 thin optical sections along the z-axis with a 1-μm step size using a 40X objective lens. The tissue volume size was 260.6 μm × 260.6 μm × 40 μm. A total of 64 images were acquired from non-overlapping fields. A single composite three-dimensional image was reconstructed using Olympus FV5700 image-analysis software. To quantify PNNs/axon in tissue samples, all CS-56/WFA-positive or 5-HT-positive images acquired from the LSCM were analyzed with the FV5700 image-analysis software. Briefly, the single composite three-dimensional image dimensions given above were reconstructed from the distribution of CS-56/WFA or 5-HT immunostaining. After the volume was thresholded by a gray level of 120, three-dimensional objects were determined from the remaining voxels. A voxel was included in an object if a face, side, edge, or corner touched any voxel already in that object. The size of a three-dimensional object was the number of voxels contained in the object. All three-dimensional objects with fewer than two voxels were eliminated from further analysis. The total volume of CS-56/WFA or 5-HT staining present in the rendered cube of tissue was then calculated in mm^3 and was divided by the total tissue volume to determine the percentage of tissue volume that was fluorescently marked. **15 slices per animal were used for quantification.**

Neurologic-function scores

Motor function was evaluated with the modified Tarlov-grading system to study the effect of LDI treatment (Rabinowitz et al. 2008). Before the surgery, the animals were trained for one week, and baseline scores were first established prior to SCI. Open-field locomotor testing was performed by two examiners, who were blinded to the study, at 1, 3, 7, 14, 30 and 60 days post-injury post-SCI using the following five-point modified Tarlov-grading system, as previously described(Rabinowitz et al. 2008): 1 - flaccid hind limbs; 2 - purposeful hind-limb motion; 3 - stands unassisted; 4 - full ambulation; and 5 – climbs at a 20° incline. Each dog was monitored from the ipsilateral side and back for a minimum of 10 walking steps. Dogs that could not bear weight on their pelvic limbs were also recorded when supported by holding the base of their tail to allow non-weight-bearing voluntary movements of their pelvic limbs to be seen. All open-field locomotor testing was performed under the same conditions and at the same time period on each scheduled testing date.

Statistical analysis

All the data were expressed as the means ± SEMs, and analyzed using the SPSS 11.0 statistical software. **Normality was counted by Shapiro-Wilk test and Kolmogorov-Smirnov test, variance homogeneity was counted by Levene's Test (see supplemental 1). Statistical analysis was evaluated by one-way analysis of variance (ANOVA) followed by Tukey's** post-hoc **test or repeated measures ANOVA with Greenhouse-Geisser adjustment.** Differences were considered statistically significant at $P < 0.05$.

Results

The temporal expression and cellular localization of CS-A and CS-C proximal to the lesion following SCI.

In the present study, we first examined the expression of CS-A and CS-C moiety of CSPGs proximal to the lesion following SCI via immunofluorescent staining. Compared to very low levels of reactivity for CS-A in the sham-operated group, we found immediately increased staining for CS-A proximal to the lesion at 1-day post-SCI that reached a peak at 14-days post-SCI. Moreover, upregulated CS-A was detected far out as 60-days post-SCI. Next, we found that LDI treatment restored the expression of CS-A to a level near that of the sham-operated group (Fig. 1A). Immunohistochemical analysis showed that, at 1-day post-SCI, 6.0 ± 1.33 cells/cm^2 were immunoreactive for CS-A in the sham-operated group, which increased to 16.3 ± 2.78 cells/cm^2 in the SCI group and was attenuated to 10.02 ± 0.98 cells/cm^2 after LDI treatment **(F (2, 12) = 7.12, p = 0.009)**. At 14-days post-SCI, the CS-A expression level was 6.2 ± 1.58 cells/cm^2 in the sham-operated group, which was increased to 32.7 ± 5.35 cells/cm^2 in SCI group and was attenuated to 15.3 ± 2.19 cells/cm^2 after LDI treatment **(F (2, 12) = 7.39, p = 0.008)**.

The temporal expression of CS-C was different from that of CS-A. Our results demonstrated that no significant variation in CS-C expression was found among the sham-operated, SCI and LDI treatment groups at 1-day post-SCI. However, CS-C was increased by 14-days post-SCI and reached a peak by 60-days post-SCI. Strikingly, in contrast to the results of CS-A expression, LDI treatment showed no inhibitory effect on CS-C expression following SCI (Fig. 1B). Immunohistochemical analysis showed that 5.8 ± 2.23 cells/cm^2 were immunoreactive for CS-C in the sham-operated group, which increased to 13.3 ± 3.27 cells/cm^2 at 14-days post-SCI in the SCI group and was similarly 12.1 ± 1.88 cells/cm^2 after LDI treatment **(F (2, 12) = 7.59, p = 0.007)**. At a later time point, there were 6.1 ± 1.09 cells/cm^2 in the sham-operated group, which was increased to 35.38 ± 2.29 cells/cm^2 at 60-days post-SCI in SCI group and was similarly 33.51 ± 1.97 cells/cm^2 after LDI treatment **(F (2, 12) = 7.62, p = 0.007)**.

We next determined the spatial expression of CS-A and CS-C proximal to the lesion. Double-immunofluorescent staining was performed with the following specific antibodies at the time points when CS-A and CS-C expressions reached their corresponding peaks: GFAP for astrocytes; MAP-2 for neurons and axons; LY111 for CS-A; and MC21 for CS-C. At 14-days post-SCI, we found substantial staining for CS-A proximal to the lesion, and colocalization of CS-A and GFAP was also apparent. On the contrary, a thin expression of CS-A was observed in MAP-2 positive neurons/axons (Fig. 1C). At 14-days post-SCI, the percentage of CS-A-positive astrocytes was 8.7 ± 0.93% in the sham-operated group, which increased to 26.8 ± 2.09% after SCI **(F (1,8) = 12.81, p = 0.000)**; the percentage of CS-A-positive neurons/axons was 5.5 ± 0.86% in the sham-operated group, which was similarly 5.8 ± 0.79% after SCI **(F (1,8) = 1.25, p = 0.100)**. At 60-days post-SCI, CS-C was upregulated in both astrocytes and neurons/axons proximal to the lesion. The percentage of CS-C positive astrocytes was 5.5 ± 0.73% in the sham-operated group, which increased to 12.2 ± 1.29% after SCI **(F (1,8) = 10.82, p = 0.000)**; the percentage of CS-C positive neurons/axons was 7.5 ± 1.29% in the sham-operated group, which was increased to 39.8 ± 1.28% after SCI **(F (1,8) = 1.35, p = 0.118)**.

LDI decreases astrocyte-associated CS-A expression, restrains CS-A-enriched PNN accumulation.

We had demonstrated that LDI inhibited CS-A expression, but not CS-C expression, proximal to the lesion following SCI. However, since CS-A is expressed in both astrocytes and neurons, we next explored whether LDI inhibits neuron-associated CS-A expression and/or astrocyte-associated CS-A expression at 14-days and 60-days post-SCI. There were rare CS-A positive neuron/axon in the sham-operated and SCI animals. LDI treatment did not alter CS-A expression in neuron/axon. At 14-days post-SCI, 3.2 ± 0.38% of neuron/axon were CS-A positive in the sham-operated group, which was similarly 3.7 ± 0.35% in the SCI group and 3.3 ± 0.02% after LDI treatment **(F (2, 12) = 1.55, p = 0.252)**. At 60-days post-SCI, 3.5 ± 0.17% of neuron/axon were CS-A positive in the sham-operated group, which was similarly 3.8 ± 0.25% in the SCI group and 3.6 ± 0.55% after LDI treatment **(F (2, 12) = 1.62, p = 0.238)** (Fig. 2B). In contrast, LDI treatment significantly inhibited CS-A expression in astrocytes. At 14-days post-SCI ,1.2 ± 0.58% of astrocytes were CS-A positive in the sham-operated group, which increased to 35.3 ± 3.26% in the SCI group and was attenuated to 5.1 ± 0.91% after LDI treatment **(F (2, 12) = 7.99, p = 0.006)**. At 60-days post-SCI, 1.5 ± 0.61% of astrocytes were CS-A positive in the sham-operated group, which increased to 39.8 ± 2.15% in the SCI group and was attenuated to 6.3 ± 1.03% after LDI treatment **(F (2, 12) = 7.85, p = 0.007)** (Fig. 2A). These results revealed that SCI increased astrocytic but not neuronal CS-A expression, and that LDI treatment induced significant inhibition of the aberrantly elevated astrocytic CS-A expression following SCI, but did not significantly affect the already stable neuronal CS-A expression in neurons following SCI.

We further used double-immunofluorescent staining and Western blotting to examine whether protein expression of C4ST-1 changed in the spinal cord tissue proximal to the lesion after LDI treatment. C4ST-1 expression was significantly increased in astrocytes following SCI in the spinal cord tissue proximal to the lesion compared to a time-matched sham-operated group (Fig. 2C) (see supplemental 2). Interestingly, after LDI treatment, C4ST-1 expression in astrocytes was significantly reduced to a level close to that of the sham-operated group. Additionally, double-immunofluorescent staining showed that 7.0 ± 0.78% of astrocytes were C4ST-1 positive in the sham-operated group, which increased to 20.5 ± 2.37% in the SCI group and was attenuated to 9.12 ± 0.56% after LDI treatment at 14-days post-SCI **(F (2, 12) = 8.01, p = 0.006)**. Later, at 60-days post-SCI, 7.2 ± 0.83% of astrocytes were C4ST-1 positive in the sham-operated group, which was increased to 19.5 ± 1.17% in SCI group and was attenuated to 9.06 ± 0.88% after LDI treatment **(F (2, 12) = 7.89, p = 0.006)**. Complementing these results, Western blotting showed that, in the SCI group, the protein expression of C4ST-1 increased to 213.5 ± 7.36% (14-days post-SCI) and 153.9 ± 5.61% (60-days post-SCI) compared to those of time-matched sham-operated animals, and LDI treatment restored the C4ST-1 protein expression to 136.3 ± 3.95% (14-days post-SCI) **(F (2, 12) = 8.06, p = 0.006)** and 120.9 ± 7.33% (60-days post-SCI) **(F (2, 12) = 8.13, p = 0.005)** of that of the sham-operated levels, respectively (Fig. 2D) (see supplemental 2).

We further investigated whether LDI treatment altered CS-A or CS-C-enriched PNNs following SCI. We used WFA to label CS-A-enriched PNNs, a CS56 antibody to label CS-C-enriched PNNs, and we quantitatively analyzed the CS-A/CS-C-enriched PNNs. We found that LDI decreased CS-A-enriched PNNs proximal to the lesion following SCI (Fig. 3A). At 14-days post-SCI, 6.3 ± 1.12% of PNNs were CS-A-

enriched in the sham-operated group, which was increased to 29.3 ± 3.32% in SCI group and was attenuated to 8.85 ± 0.96% after LDI treatment **(F (2, 12) = 7.93, p = 0.006)**. At 60-days post-SCI, 6.7 ± 1.07% of PNNs were CS-A-enriched in the sham-operated group, which was increased to 35.3 ± 1.89% in SCI group and was attenuated to 9.27 ± 1.03% after LDI treatment **(F (2, 12) = 7.79, p = 0.007)**. However, LDI treatment had no significant inhibitory effect on CS-C-enriched PNNs expression. At 14-days post-SCI, 5.8 ± 0.89% of PNNs were CS-C-enriched in the sham-operated group, which increased to 22.5 ± 1.28% in the SCI group and was 19.25 ± 1.53% after LDI treatment **(F (2, 12) = 1.89, p = 0.193**). At 60-days post-SCI, 6.2 ± 1.01% of PNNs were CS-C-enriched in the sham-operated group, which increased to 31.5 ± 1.75% in the SCI group and was 28.2 ± 1.19% after LDI treatment **(F (2, 12) = 1.92, p = 0.189)** (Fig. 3B).

LDI increases expression of 5-HT axons accompanied with reduction of CS-A-enriched PNNs

Using laser-scanning confocal microscopy and different fluorescent probes, we measured 5-HT axonal sprouting and CS-A-enriched/CS-C-enriched PNNs accumulation by three-dimensional image acquisition and reconstruction in sham-operated, SCI and LDI groups. Three-dimensional reconstructed images showed that prominent CS-A-enriched PNNs and CS-C-enriched PNNs surrounded axons with decreased 5-HT positive axons on the ipsilateral side following SCI when compared to that of the sham-operated group. LDI treatment reversed 5-HT-positive axonal spouting and decreased CS-A-enriched PNNs accumulation, but no inhibitory effect on CS-C-enriched PNNs.

We first measured the percentage of 5-HT axons/tissue and CS-A-enriched PNNs/tissue. At 14-days post-SCI, in the sham-operated group, the percentage of 5-HT axons/tissue was 29.6 ± 0.67%, the percentage of CS-A-enriched PNNs/tissue was 6.3 ± 1.12%; in the SCI group, 5-HT axons were repelled in a similar manner between CS-A-enriched PNNs proximal to the lesion, and the percentage of 5-HT axons/tissue was reduced to 5.1 ± 0.79%, the percentage of CS-A-enriched PNNs/tissue was 29.3 ± 3.32%; following LDI treatment, the percentage of 5-HT axons/tissue was increased to 25.2 ± 1.08%, the percentage of CS-A-enriched PNNs/tissue was 8.85 ± 0.96% (Fig. 3). At 60-days post-SCI, decreased 5-HT axon also accompanied with increased CS-A-enriched PNNs. In sham-operated group, the percentage of 5-HT axons/tissue was 28.3 ± 1.05%, the percentage of CS-A-enriched PNNs/tissue was 6.7 ± 1.07%; in SCI group, the percentage of 5-HT axons/tissue was 6.5 ± 0.82%, the percentage of CS-A-enriched PNNs/tissue was 35.3 ± 1.89%; in LDI group, the percentage of 5-HT axons/tissue was 25.5 ± 1.06%, the percentage of CS-A-enriched PNNs/tissue was 9.27 ± 1.03%.

The percentage of 5-HT axons/tissue and CS-C-enriched PNNs/tissue were also measured. At 14-days post-SCI, in the sham-operated group, the percentage of 5-HT axons/tissue was 27.3 ± 0.85%, the percentage of CS-C-enriched PNNs/tissue was 6.2 ± 0.97%; in the SCI group, the percentage of 5-HT axons/tissue was reduced to 7.5 ± 0.39%, the percentage of CS-C-enriched PNNs/tissue was 28.1 ± 1.15%; following LDI treatment, the percentage of 5-HT axons/tissue was increased to 10.3 ± 1.22%, the percentage of CS-C-enriched PNNs/tissue was 25.2 ± 0.96%. At 60-days post-SCI, in sham-operated group, the percentage of 5-HT axons/tissue was 23.8 ± 1.13%, the percentage of CS-C-enriched PNNs/tissue was

6.6 ± 1.10%; in SCI group, the percentage of 5-HT axons/tissue was 7.3 ± 1.01%, the percentage of CS-C-enriched PNNs/tissue was 36.3 ± 1.77%; in LDI group, the percentage of 5-HT axons/tissue was 11.2 ± 1.63%, the percentage of CS-C-enriched PNNs/tissue was 32.2 ± 0.89%.

We further analyzed the correlation between of 5-HT axonal immunoreactivity and CS-A/CS-C-enriched PNNs immunoreactivity through Pearson correlation following LDI treatment. There was a significant correlation between a reduction of CS-A-enriched PNNs and an increase of 5-HT axonal immunoreactivity (r^2 = 0.810 at 14-days post-SCI, r^2 = 0.706 at 60-days post-SCI, $P < 0.05$), but no significant correlation between change of CS-C-enriched PNNs and an increase of 5-HT axonal immunoreactivity (r^2 = 0.050 at 14-days post-SCI, r^2 = 0.249 at 60-days post-SCI, $P > 0.05$).

LDI increases 5-HT receptor expression but does not affect Nogo receptors, RPTPσ or LAR expression following SCI.

In order to identify the effect of LDI treatment on functional receptors of CSPGs and 5-HT receptors, we compared the expression levels of 5-HT receptors, Nogo receptors, RPTPσ and LAR in neurons through double-immunofluorescent staining in the sham, SCI and LDI groups.

As shown in Fig. 4, the sham-operated group showed a very weak expression of 5-$HT_{2c/a}$ and 5-HT_7, and these expression levels were similar in the SCI group. In contrast, the LDI group showed a significantly increased expression of 5-HT_{2A}, 5-HT_{2C} and 5-HT_7 in neurons (Fig. 4). The percentage of 5-$HT_{2c/a}$-positive neurons was 12.5 ± 1.08% in the sham-operated group, 18.2 ± 2.16% in the SCI group, and was increased to 26.7 ± 1.67% in the LDI group **($F(2, 12) = 8.65, p = 0.005$)**. Similarly, the percentage of 5-HT_7-positive neurons was 11.7 ± 0.88% in the sham-operated group, 18.6 ± 1.03% in the SCI group, and was increased to 27.3 ± 1.25% in the LDI group **($F(2, 12) = 8.82, p = 0.004$)**.

We next investigated to what extent LDI could be involved in the regulation of the Nogo receptors, NgR1 and NgR3. The sham-operated group only showed minimal expression of NgR1 and NgR3 in neurons. In comparison to the sham-operated group, the SCI group showed an increased expression of NgR1 and NgR3 in neurons. There was no significant difference in the expression of NgR1 or NgR3 in neurons between the SCI group and LDI group (Fig. 5A,C). The percentage of NgR1-positive neurons was 8.3 ± 0.58% in the sham-operated group, 9.3 ± 0.86% in the SCI group, and 9.8 ± 0.67% in the LDI group **($F(2, 12) = 1.58, p = 0.250$)**. The percentage of NgR3-positive neurons was 8.5 ± 0.63% in the sham-operated group, 9.6 ± 0.59% in the SCI group, and 10.1 ± 0.82% in the LDI group **($F(2, 12) = 1.32, p = 0.303$)**.

We also measured the expression of RPTP-σ and LAR in neurons. Similar to the expression of NgR1 and NgR3, there was no significant difference in the expression of RPTP-σ or LAR in neurons between the SCI group and LDI group (Fig. 5B, D). The percentage of RPTP-σ-positive neurons was 6.8 ± 0.56% in the sham-operated group and increased to 15.8 ± 1.01% in the SCI group and 16.2 ± 1.67% in the LDI group **($F(2, 12) = 1.01, p = 0.393$)**. The percentage of LAR-positive neurons was 5.9 ± 0.63% in the sham-operated

group and increased to 22.9 ± 1.58% in the SCI group and 23.7 ± 1.33% in the LDI group **(F (2, 12) = 0.83, p = 0.459)**.

LDI promotes motor function recovery following SCI.

The modified-Tarlov grading system was used to test hindlimb motor-function. The motor function of the hindlimbs was intact before SCI. After SCI, the injured side lower limbs were paralysis (Tarlov Grade 1) and incontinent, which suggested a severe and consistent lesion. After injury, serious hindlimb paralysis with no residual motor function was observed in all dogs, and hindlimb scores neared zero. At 7 days post-injury, some animals regained a slight improvement for weight support due to spontaneous recovery. Compared to SCI-treated animals, enhanced hindlimb motor-function recovery occurred in the LDI-treated animals. At 14 days post-SCI, the modified Tarlov scale in the sham-operated group was 5(0); this level decreased to 3(0) in the SCI group and was ameliorated to 3(1) with LDI treatment **(F (2, 12) = 10.67, p = 0.002)**; At 60 days post-SCI, the modified Tarlov scale in the sham-operated group was 5(0); this level decreased to 3(1) in the SCI group and was ameliorated to 4(0) with LDI treatment **(F (2, 12) = 10.25, p = 0.002)** (Fig. 6). These data suggest that LDI treatment improved hindlimb motor-function recovery after SCI.

Discussion

In this study, we show that specific sulfation patterns of CSs moieties play different role in modulation of axon re-growth in a canine SCI model. Upregulated CS-A expression occurred at 1-day post-SCI, earlier than CS-C which was increased at 14-days post-SCI. CS-A was mainly colocalized with astrocytes but CS-C was upregulated in both astrocytes and neurons/axons. LDI significantly inhibited the expressions of astrocyte-associated CS-A and CS-A-enriched PNNs, but no inhibitory effect on CS-C and CS-C-enriched PNNs. There was a significant correlation between a reduction of CS-A-enriched PNNs and an increase of serotonergic (5-hydroxytryptamine, 5-HT) axonal sprouting. Increased serotonergic axon sprouting proximal to the lesion could be enhanced via 5HT receptor inducing following LDI treatment. Furthermore, LDI treatment promoted hindlimb motor function recovery following SCI.

Translational therapy for SCI, from laboratory to clinic, has been highlighting the suitable animal models which mirrored human conditions. Dogs' spinal cords more closely resemble humans' than do those in rodent species, including genetic similarities, similar caliber/length of the spinal cord, similarity of biological responses to SCI (such as inflammatory reaction); and more human-like spontaneous recovery (Jeffery et al. 2006; Webb et al. 2004). Dogs' larger sized cord mimics the changes in human SCI, specifically in axonal sprouting across glial scars. In addition, pathophysiological investigations and neurological function examinations can be carried out easily in dog (including histopathology examination, MRI, evoked potentials, and functional outcome scores) (Jeffery et al. 2020). There are also several potential disadvantages including ethical concerns and high operating costs. Therefore, we strictly applied the principle of the 3Rs (replacement, reduction, refinement) to reduce the number of

animals used in experiments as far as possible, to refine the pain and distress to which animals are exposed. We also explored some special methods suitable for beagle dogs postoperative care.

Previous studies have shown that CSPGs inhibit axonal regeneration. However, the importance of specific sulfation patterns of CSs moieties to axon regeneration might have been overlooked in previous studies, because some treatments, as represented by chondroitinase ABC, destroy all CSs moieties. Following CNS injury, there is a large overall increase in CS moieties, many studies shown different changes in the patterns of sulfation. Upregulation of CS-A, but not CS-C, is found in spinal cord tissue following SCI (Properzi et al. 2005; Wang et al. 2008). In contrast, CS-C and C6ST-1 (key enzymes for CS-C Synthesis) are upregulated following cortical-stab injury in the mouse cerebral cortex (Properzi et al. 2005; Yin et al. 2009; Yutsudo and Kitagawa 2015). The expression imbalance of CSs moieties around the lesion site might be a determining factor for axonal regeneration. Previous studies showed that CS-A and CS-C have different effects on plasticity, CS-C was beneficial to axon regeneration, while CS-A was inhibitory (Bhattacharyya et al. 2009; Yoo et al. 2013; Pearson et al. 2018). Our present results showed that, in beagle dogs, CS-A and CS-C moieties increased at different time points. In our present study, CS-A immediately increased, reached a peak at 14-days and still be observed at 60-days post-SCI. In contrast, CS-C increased at 14-days and reached a peak at 60-days post-SCI. In addition, CS-A was mainly expressed in astrocytes, while CS-C was expressed in neuron/axons and astrocytes following SCI. The different temporal and spatial expressions of CSs in the CNS might offer promising therapeutic time windows or targets.

Our study further demonstrated that, after LDI treatment, astrocytes associated CS-A dramatically decreased proximal to the lesion, but this tendency was not shown in astrocytes associated CS-C, neurons associated CS-A and neurons associated CS-C in the same place. Our early administration of LDI (LDI treatment was performed beginning at 1-day post-SCI) largely inhibit the expression of astrocytes associated CS-A following SCI, potentially decreased astrocyte activation and reduced release of astrocyte associated cytokines. More important, continuous LDI intervention (the irradiation was continuous performed for 14 days) induced a durable and specific elimination during the peak period of astrocyte-associated CS-A expression. By contrast, transient intervention of CSPG often yields undesirable effects. A recent study showed that single administration of chondroitinase ABC transient increased pericontusional grey and white matter sprouting in the rat cortex, but no continuous motor function recovery; the transient effects of CSPG cleavage also accompanied with the delayed CS moieties upregulation and a decline in neuroplasticity (Harris et al. 2010). LDI could inhibited astrocytes and microglia proliferation following SCI (Zhang et al. 2017). Moreover, early modulation cell-cycle of astrocytes and microglia reduced the levels of inhibitory molecules for axonal regeneration (Zhang et al. 2009; Wang et al. 2009). Therefore, the possible reason why LDI specific inhibited the CS-A and had little effect on CS-C was as follows: 1.LDI treatment inhibited astrocytes activation/proliferation following SCI, the CS-A level decreased due to reducing the number and activity of astrocytes. 2. During CS-A biosynthesis, GalNAc residues of the repeating disaccharide units are sulfated at C4 by C4ST-1, the key synthesis enzyme of CS-A. In this study, LDI inhibited the expression of C4ST-1, which led to the decrease of CS-A expression. 3. The inhibition of astrocyte activation block the secondary inflammatory reaction

(activation/migration of microglia and macrophages, and release of a large number of inflammatory factors), which reaction further enhanced astrocytes activation/proliferation.

CSPGs recruit adhesion molecules and growth factors to their cognate receptors (Leadbeater et al. 2006). These co-receptor functions are important for axonal growth and guidance (Hacker et al. 2005), and these co-receptors (Nogo receptors and LAR-RPTPs) show different affinities to CS moieties of CSPGs. For example, NgR1 and NgR3, the Nogo receptors, showed high-affinity activity to CS-B, CS-D and CS-E (Brown et al. 2012; Mironova and Giger 2013); and RPTPσ strongly bind with CS-D and CS-E (Yi et al. 2014). In our present study, the expression level of CSPGs receptors (Nogo-receptor, RPTPσ or LAR) showed no significant difference between SCI and LDI group. Another kind of receptors, 5-$HT_{2c/a}$ and 5-HT_7, showed increased levels in LDI treatment group. The increased 5-$HT_{2c/a}$ and 5-HT_7 expression might be an enhanced compensatory mechanism for serotonergic axon sprouting following LDI treatment.

The locomotion dysfunction following SCI can be attributed considerably to the loss of descending 5-HT pathways. Previous studies have also demonstrated that increased sprouting of 5-HT fibers promoted locomotor functional recovery (Tom et al. 2009; Warren et al. 2018). Promotion of 5-HT axonal regeneration after spinal cord injury might be a promising treatment. In this study, the increased expression of 5-HT axons and 5-HT receptors, in the LDI treatment group, might be the major positive factor for locomotor recovery.

Our three-dimensional image acquisition and reconstruction also showed that there was a significant correlation between a reduction of CS-A-enriched PNNs and an increase of 5-HT axonal immunoreactivity, but no correlation between change of CS-C-enriched PNNs and 5-HT axonal immunoreactivity. After SCI, some residual axons attempted to reconstruct neuron circuit. However, due to lacking of guidance mechanisms, these residual axons mostly connected to wrong targets and became dystrophic endbulbs, resulted in poor limb motor function (Hill 2017; Young 2014). By eliminating PNNs, chondroitinase ABC showed neuroplasticity and allows recovery of skilled paw-reaching functionality (Tom et al. 2009). If the downregulation of CS-A-enriched PNNs leads to an increase in CNS plasticity, we would therefore expect that LDI treatment would recover limb motor function after nerve repair. As expected, the LDI treatment animals showed efficacious recovery over the entire experimental period, indicating a high level of spinal cord plasticity.

Taken together, our findings show that specific sulfation patterns along the carbohydrate backbone of CSPGS and CSPG-enriched PNNs involved in carrying instructions for regulating axonal regeneration. LDI provided a highway for axon regeneration while inducing reinnervation of axonal targets. Therefore, LDI treatment may be an efficacious strategy for treating SCI.

Declarations

ACKNOWLEDGMENTS

The investigations were supported by National Natural Science Foundation of China (81471230, 30900450 to Qiang Zhang, 81601480 to Ying Xiong and 91332108 to Wei Wang).We thank LetPub (www.letpub.com) for its linguistic assistance during the preparation of this manuscript.

AUTHOR CONTRIBUTION

Q.Z and W.W designed the research. Q.Z, Y.X and Bo.Z conducted the research. Y.X, J.X and Bi. Z analyzed and interpreted the data. Q.Z and Y.X wrote the manuscript.

DECLARATION OF COMPETING INTEREST

Authors confirm that they have no conflicts of interest related with the preset study.

References

1. Akbik F, Cafferty WB, Strittmatter SM (2012) Myelin associated inhibitors: a link between injury-induced and experience-dependent plasticity. Exp Neurol 235(1):43–52. doi:10.1016/j.expneurol.2011.06.006
2. Azria D, Betz M, Bourgier C, Jeanneret Sozzi W, Ozsahin M (2012) Identifying patients at risk for late radiation-induced toxicity. Crit Rev Oncol Hematol 84 Suppl 1:e35–e41. doi:10.1016/j.critrevonc.2010.08.003
3. Banerjee SB, Gutzeit VA, Baman J, Aoued HS, Doshi NK, Liu RC, Ressler KJ (2017) Perineuronal Nets in the Adult Sensory Cortex Are Necessary for Fear Learning. Neuron 95(1):169–179 e163. doi:10.1016/j.neuron.2017.06.007
4. Beurdeley M, Spatazza J, Lee HH, Sugiyama S, Bernard C, Di Nardo AA, Hensch TK, Prochiantz A (2012) Otx2 binding to perineuronal nets persistently regulates plasticity in the mature visual cortex. J Neurosci 32(27):9429–9437. doi:10.1523/JNEUROSCI.0394-12.2012
5. Bhattacharyya S, Solakyildirim K, Zhang Z, Linhardt RJ, Tobacman JK (2009) Chloroquine reduces arylsulphatase B activity and increases chondroitin-4-sulphate: implications for mechanisms of action and resistance. Malar J 8:303. doi:10.1186/1475-2875-8-303
6. Bradbury EJ, Moon LD, Popat RJ, King VR, Bennett GS, Patel PN, Fawcett JW, McMahon SB (2002) Chondroitinase ABC promotes functional recovery after spinal cord injury. Nature 416(6881):636–640. doi:10.1038/416636a
7. Brown JM, Xia J, Zhuang B, Cho KS, Rogers CJ, Gama CI, Rawat M, Tully SE, Uetani N, Mason DE, Tremblay ML, Peters EC, Habuchi O, Chen DF, Hsieh-Wilson LC (2012) A sulfated carbohydrate epitope inhibits axon regeneration after injury. Proc Natl Acad Sci U S A 109(13):4768–4773. doi:10.1073/pnas.1121318109
8. Dickendesher TL, Baldwin KT, Mironova YA, Koriyama Y, Raiker SJ, Askew KL, Wood A, Geoffroy CG, Zheng B, Liepmann CD, Katagiri Y, Benowitz LI, Geller HM, Giger RJ (2012) NgR1 and NgR3 are receptors for chondroitin sulfate proteoglycans. Nat Neurosci 15(5):703–712. doi:10.1038/nn.3070

9. Doperalski AE, Montgomery LR, Mondello SE, Howland DR (2020) Anatomical Plasticity of Rostrally Terminating Axons as a Possible Bridging Substrate across a Spinal Injury. J Neurotrauma 37(6):877–888. doi:10.1089/neu.2018.6193
10. Dyck SM, Alizadeh A, Santhosh KT, Proulx EH, Wu CL, Karimi-Abdolrezaee S (2015) Chondroitin Sulfate Proteoglycans Negatively Modulate Spinal Cord Neural Precursor Cells by Signaling Through LAR and RPTPsigma and Modulation of the Rho/ROCK Pathway. Stem Cells 33(8):2550–2563. doi:10.1002/stem.1979
11. Fawcett JW, Oohashi T, Pizzorusso T (2019) The roles of perineuronal nets and the perinodal extracellular matrix in neuronal function. Nat Rev Neurosci 20(8):451–465. doi:10.1038/s41583-019-0196-3
12. Fink KL, Lopez-Giraldez F, Kim IJ, Strittmatter SM, Cafferty WBJ (2017) Identification of Intrinsic Axon Growth Modulators for Intact CNS Neurons after Injury. Cell Rep 18(11):2687–2701. doi:10.1016/j.celrep.2017.02.058
13. Fisher D, Xing B, Dill J, Li H, Hoang HH, Zhao Z, Yang XL, Bachoo R, Cannon S, Longo FM, Sheng M, Silver J, Li S (2011) Leukocyte common antigen-related phosphatase is a functional receptor for chondroitin sulfate proteoglycan axon growth inhibitors. J Neurosci 31(40):14051–14066. doi:10.1523/JNEUROSCI.1737-11.2011
14. Goya S, Wada T, Shimada K, Hirao D, Tanaka R (2018) Dose-dependent effects of isoflurane and dobutamine on cardiovascular function in dogs with experimental mitral regurgitation. Vet Anaesth Analg 45(4):432–442. doi:10.1016/j.vaa.2018.03.010
15. Hacker U, Nybakken K, Perrimon N (2005) Heparan sulphate proteoglycans: the sweet side of development. Nat Rev Mol Cell Biol 6(7):530–541. doi:10.1038/nrm1681
16. Harris NG, Mironova YA, Hovda DA, Sutton RL (2010) Chondroitinase ABC enhances pericontusion axonal sprouting but does not confer robust improvements in behavioral recovery. J Neurotrauma 27(11):1971–1982. doi:10.1089/neu.2010.1470
17. Hill CE (2017) A view from the ending: Axonal dieback and regeneration following SCI. Neurosci Lett 652:11–24. doi:10.1016/j.neulet.2016.11.002
18. Hou X, Yoshioka N, Tsukano H, Sakai A, Miyata S, Watanabe Y, Yanagawa Y, Sakimura K, Takeuchi K, Kitagawa H, Hensch TK, Shibuki K, Igarashi M, Sugiyama S (2017) Chondroitin Sulfate Is Required for Onset and Offset of Critical Period Plasticity in Visual Cortex. Sci Rep 7(1):12646. doi:10.1038/s41598-017-04007-x
19. Jefferson SC, Tester NJ, Howland DR (2011) Chondroitinase ABC promotes recovery of adaptive limb movements and enhances axonal growth caudal to a spinal hemisection. J Neurosci 31(15):5710–5720. doi:10.1523/JNEUROSCI.4459-10.2011
20. Jeffery ND, Mankin JM, Ito D, Boudreau CE, Kerwin SC, Levine JM, Krasnow MS, Andruzzi MN, Alcott CJ, Granger N (2020) Extended durotomy to treat severe spinal cord injury after acute thoracolumbar disc herniation in dogs. Vet Surg. doi:10.1111/vsu.13423

21. Jeffery ND, Smith PM, Lakatos A, Ibanez C, Ito D, Franklin RJ (2006) Clinical canine spinal cord injury provides an opportunity to examine the issues in translating laboratory techniques into practical therapy. Spinal Cord 44(10):584–593. doi:10.1038/sj.sc.3101912
22. Jeffrey PR, Nhat-Thi Vo,Alvaro Sagasti (2018) Fish Scales Dictate the Pattern of Adult Skin Innervation and Vascularization. Dev Cell 46(3):344–359.e4. doi:10.1016/j.devcel.2018.06.019
23. Jung-Yu C, Hsu,Robert McKeon,Staci Goussev,Zena Werb,Jung-Uek Lee,Alpa Trivedi,Linda J, Noble-Haeusslein (2006) Matrix metalloproteinase-2 facilitates wound healing events that promote functional recovery after spinal cord injury. J Neurosci,26(39):9841-50. doi: 10.1523/JNEUROSCI.1993-06.2006
24. Khan DC, Malhotra S, Stevens RE, Steinfeld AD (1999) Radiotherapy for the treatment of giant cell tumor of the spine: a report of six cases and review of the literature. Cancer Invest 17(2):110–113
25. Kim JS, Yang M, Kim SH, Shin T, Moon C (2013) Neurobiological toxicity of radiation in hippocampal cells. Histol Histopathol 28(3):301–310. doi:10.14670/HH-28.301
26. Koshman YE, Herzberg BR, Seifert TR, Polakowski JS, Mittelstadt SW (2018) The evaluation of drug-induced changes in left ventricular function in pentobarbital-anesthetized dogs. J Pharmacol Toxicol Methods 91:27–35. doi:10.1016/j.vascn.2018.01.002
27. Kurihara D, Yamashita T (2012) Chondroitin sulfate proteoglycans down-regulate spine formation in cortical neurons by targeting tropomyosin-related kinase B (TrkB) protein. J Biol Chem 287(17):13822–13828. doi:10.1074/jbc.M111.314070
28. Lang BT, Cregg JM, DePaul MA, Tran AP, Xu K, Dyck SM, Madalena KM, Brown BP, Weng YL, Li S, Karimi-Abdolrezaee S, Busch SA, Shen Y, Silver J (2015) Modulation of the proteoglycan receptor PTPsigma promotes recovery after spinal cord injury. Nature 518(7539):404–408. doi:10.1038/nature13974
29. Leadbeater WE, Gonzalez AM, Logaras N, Berry M, Turnbull JE, Logan A (2006) Intracellular trafficking in neurones and glia of fibroblast growth factor-2, fibroblast growth factor receptor 1 and heparan sulphate proteoglycans in the injured adult rat cerebral cortex. J Neurochem 96(4):1189–1200. doi:10.1111/j.1471-4159.2005.03632.x
30. Lee H, McKeon RJ, Bellamkonda RV (2010) Sustained delivery of thermostabilized chABC enhances axonal sprouting and functional recovery after spinal cord injury. Proc Natl Acad Sci U S A 107(8):3340–3345. doi:10.1073/pnas.0905437106
31. LeRoux LG, Bredow S, Grosshans D, Schellingerhout D (2014) Molecular imaging detects impairment in the retrograde axonal transport mechanism after radiation-induced spinal cord injury. Mol Imaging Biol 16(4):504–510. doi:10.1007/s11307-013-0713-0
32. Marcus RB Jr, Million RR (1990) The incidence of myelitis after irradiation of the cervical spinal cord. Int J Radiat Oncol Biol Phys 19(1):3–8. doi:10.1016/0360-3016(90)90126-5
33. Masu M (2016) Proteoglycans and axon guidance: a new relationship between old partners. J Neurochem 139 Suppl 2:58–75. doi:10.1111/jnc.13508

34. Mattias ND, Svensson,Martina Zoccheddu,Shen Yang,Gyrid Nygaard,Christian Secchi,Karen MD,Kamil Slowikowski,Fumitaka Mizoguchi,Frances Humby,Rebecca Hands,Eugenio Santelli,Cristiano Sacchetti,Kuninobu Wakabayashi,Dennis J (2020) Synoviocyte-targeted therapy synergizes with TNF inhibition in arthritis reversal. Sci Adv,6(26):eaba4353. doi: 10.1126/sciadv.aba4353
35. Mikami T, Mizumoto S, Kago N, Kitagawa H, Sugahara K (2003) Specificities of three distinct human chondroitin/dermatan N-acetylgalactosamine 4-O-sulfotransferases demonstrated using partially desulfated dermatan sulfate as an acceptor: implication of differential roles in dermatan sulfate biosynthesis. J Biol Chem 278(38):36115–36127. doi:10.1074/jbc.M306044200
36. Mironova YA, Giger RJ (2013) Where no synapses go: gatekeepers of circuit remodeling and synaptic strength. Trends Neurosci 36(6):363–373. doi:10.1016/j.tins.2013.04.003
37. Miyata S, Kitagawa H (2015) Mechanisms for modulation of neural plasticity and axon regeneration by chondroitin sulphate. J Biochem 157(1):13–22. doi:10.1093/jb/mvu067
38. Miyata S, Komatsu Y, Yoshimura Y, Taya C, Kitagawa H (2012) Persistent cortical plasticity by upregulation of chondroitin 6-sulfation. Nat Neurosci 15(3):414–422. doi:10.1038/nn.3023 S411-412.
39. Muir E, De Winter F, Verhaagen J, Fawcett J (2019) Recent advances in the therapeutic uses of chondroitinase ABC. Exp Neurol 321:113032. doi:10.1016/j.expneurol.2019.113032
40. O'Shea TM, Burda JE, Sofroniew MV (2017) Cell biology of spinal cord injury and repair. J Clin Invest 127(9):3259–3270. doi:10.1172/JCI90608
41. Pearson CS, Mencio CP, Barber AC, Martin KR, Geller HM (2018) Identification of a critical sulfation in chondroitin that inhibits axonal regeneration. Elife 7. doi:10.7554/eLife.37139
42. Philippa M, Warren,Stephanie C, Steiger,Thomas E, Dick,Peter M, MacFarlane,Warren JA, Jerry Silver (2018) Rapid and robust restoration of breathing long after spinal cord injury. Nat Commun 9(1):4843. doi:10.1038/s41467-018-06937-0
43. Pizzorusso T, Medini P, Berardi N, Chierzi S, Fawcett JW, Maffei L (2002) Reactivation of ocular dominance plasticity in the adult visual cortex. Science 298(5596):1248–1251. doi:10.1126/science.1072699
44. Properzi F, Carulli D, Asher RA, Muir E, Camargo LM, van Kuppevelt TH, ten Dam GB, Furukawa Y, Mikami T, Sugahara K, Toida T, Geller HM, Fawcett JW (2005) Chondroitin 6-sulphate synthesis is up-regulated in injured CNS, induced by injury-related cytokines and enhanced in axon-growth inhibitory glia. Eur J Neurosci 21(2):378–390. doi:10.1111/j.1460-9568.2005.03876.x
45. Rabinowitz RS, Eck JC, Harper CM Jr, Larson DR, Jimenez MA, Parisi JE, Friedman JA, Yaszemski MJ, Currier BL (2008) Urgent surgical decompression compared to methylprednisolone for the treatment of acute spinal cord injury: a randomized prospective study in beagle dogs. Spine (Phila Pa 1976) 33(21):2260–2268. doi:10.1097/BRS.0b013e31818786db
46. Ridet JL, Pencalet P, Belcram M, Giraudeau B, Chastang C, Philippon J, Mallet J, Privat A, Schwartz L (2000) Effects of spinal cord X-irradiation on the recovery of paraplegic rats. Exp Neurol 161(1):1–

14. doi:10.1006/exnr.1999.7206

47. Schafer MKE, Tegeder I (2018) NG2/CSPG4 and progranulin in the posttraumatic glial scar. Matrix Biol 68–69:571–588. doi:10.1016/j.matbio.2017.10.002
48. Schultheiss TE (1990) Spinal cord radiation "tolerance": doctrine versus data. Int J Radiat Oncol Biol Phys 19(1):219–221. doi:10.1016/0360-3016(90)90157-f
49. Sharma R, Al-Saleem FH, Panzer J, Lee J, Puligedda RD, Felicori LF, Kattala CD, Rattelle AJ, Ippolito G, Cox RH, Lynch DR, Dessain SK (2018) Monoclonal antibodies from a patient with anti-NMDA receptor encephalitis. Ann Clin Transl Neurol 5(8):935–951. doi:10.1002/acn3.592
50. Slawinska U, Miazga K, Jordan LM (2014) The role of serotonin in the control of locomotor movements and strategies for restoring locomotion after spinal cord injury. Acta Neurobiol Exp (Wars) 74(2):172–187
51. Raha-Chowdhury,James SFoscarin,Ruma, Fawcett,Jessica W, Kwok CF (2017) Brain ageing changes proteoglycan sulfation, rendering perineuronal nets more inhibitory. Aging 9(6):1607–1622. doi:10.18632/aging.101256
52. Sorg BA, Berretta S, Blacktop JM, Fawcett JW, Kitagawa H, Kwok JC, Miquel M (2016) Casting a Wide Net: Role of Perineuronal Nets in Neural Plasticity. J Neurosci 36(45):11459–11468. doi:10.1523/JNEUROSCI.2351-16.2016
53. Sullivan CS, Gotthard I, Wyatt EV, Bongu S, Mohan V, Weinberg RJ, Maness PF (2018) Perineuronal Net Protein Neurocan Inhibits NCAM/EphA3 Repellent Signaling in GABAergic Interneurons. Sci Rep 8(1):6143. doi:10.1038/s41598-018-24272-8
54. Tester NJ, Howland DR (2008) Chondroitinase ABC improves basic and skilled locomotion in spinal cord injured cats. Exp Neurol 209(2):483–496. doi:10.1016/j.expneurol.2007.07.019
55. Tohda C, Kuboyama T (2011) Current and future therapeutic strategies for functional repair of spinal cord injury. Pharmacol Ther 132(1):57–71. doi:10.1016/j.pharmthera.2011.05.006
56. Tom VJ, Kadakia R, Santi L, Houle JD (2009) Administration of chondroitinase ABC rostral or caudal to a spinal cord injury site promotes anatomical but not functional plasticity. J Neurotrauma 26(12):2323–2333. doi:10.1089/neu.2009.1047
57. Tran AP, Warren PM, Silver J (2018) The Biology of Regeneration Failure and Success After Spinal Cord Injury. Physiol Rev 98(2):881–917. doi:10.1152/physrev.00017.2017
58. Wang H, Katagiri Y, McCann TE, Unsworth E, Goldsmith P, Yu ZX, Tan F, Santiago L, Mills EM, Wang Y, Symes AJ, Geller HM (2008) Chondroitin-4-sulfation negatively regulates axonal guidance and growth. J Cell Sci 121(Pt 18):3083–3091. doi:10.1242/jcs.032649
59. Wang W, Bu B, Xie M, Zhang M, Yu Z, Tao D (2009) Neural cell cycle dysregulation and central nervous system diseases. Prog Neurobiol 89(1):1–17. doi:10.1016/j.pneurobio.2009.01.007
60. Warren PM, Steiger SC, Dick TE, MacFarlane PM, Alilain WJ, Silver J (2018) Rapid and robust restoration of breathing long after spinal cord injury. Nat Commun 9(1):4843. doi:10.1038/s41467-018-06937-0

61. Webb AA, Jeffery ND, Olby NJ, Muir GD (2004) Behavioural analysis of the efficacy of treatments for injuries to the spinal cord in animals. Vet Rec 155(8):225–230. doi:10.1136/vr.155.8.225
62. Ye Q, Miao QL (2013) Experience-dependent development of perineuronal nets and chondroitin sulfate proteoglycan receptors in mouse visual cortex. Matrix Biol 32(6):352–363. doi:10.1016/j.matbio.2013.04.001
63. Yi JH, Katagiri Y, Yu P, Lourie J, Bangayan NJ, Symes AJ, Geller HM (2014) Receptor protein tyrosine phosphatase sigma binds to neurons in the adult mouse brain. Exp Neurol 255:12–18. doi:10.1016/j.expneurol.2014.02.007
64. Yin J, Sakamoto K, Zhang H, Ito Z, Imagama S, Kishida S, Natori T, Sawada M, Matsuyama Y, Kadomatsu K (2009) Transforming growth factor-beta1 upregulates keratan sulfate and chondroitin sulfate biosynthesis in microglias after brain injury. Brain Res 1263:10–22. doi:10.1016/j.brainres.2009.01.042
65. Yoo M, Khaled M, Gibbs KM, Kim J, Kowalewski B, Dierks T, Schachner M (2013) Arylsulfatase B improves locomotor function after mouse spinal cord injury. PLoS One 8(3):e57415. doi:10.1371/journal.pone.0057415
66. Young W (2014) Spinal cord regeneration. Cell Transplant 23(4–5):573–611. doi:10.3727/096368914X678427
67. Yutsudo N, Kitagawa H (2015) Involvement of chondroitin 6-sulfation in temporal lobe epilepsy. Exp Neurol 274 (Pt B):126–133. doi:10.1016/j.expneurol.2015.07.009
68. Zhang Q, Chen C, Lu J, Xie M, Pan D, Luo X, Yu Z, Dong Q, Wang W (2009) Cell cycle inhibition attenuates microglial proliferation and production of IL-1beta, MIP-1alpha, and NO after focal cerebral ischemia in the rat. Glia 57(8):908–920. doi:10.1002/glia.20816
69. Zhang Q, Xiong Y, Zhu B, Zhu B, Tian D, Wang W (2017) Low-dose fractionated irradiation promotes axonal regeneration beyond reactive gliosis and facilitates locomotor function recovery after spinal cord injury in beagle dogs. Eur J Neurosci 46(9):2507–2518. doi:10.1111/ejn.13714
70. Zhang ZG, Bower L, Zhang RL, Chen S, Windham JP, Chopp M (1999) Three-dimensional measurement of cerebral microvascular plasma perfusion, glial fibrillary acidic protein and microtubule associated protein-2 immunoreactivity after embolic stroke in rats: a double fluorescent labeled laser-scanning confocal microscopic study. Brain Res 844(1–2):55–66. doi:10.1016/s0006-8993(99)01886-7

Tables

Table.1 Primary antibody used in double-immunofluorescent staining

	Manufacturer	Clonality	Product code (Catalogue number)	Dilution	Reference
anti-CS56	Invitrogen	mouse monoclonal IgM	MA183055	1:200	Jeffrey et al. 2018
anti-GFAP	R&D systems	mouse monoclonal IgM	MAB2594	1:100	The specificity validated using knockout validation
anti-MAP-2	Invitrogen	mouse monoclonal IgM	13-1500	1:300	Sharma et al. 2017
anti-CS-A	Seikagaku	mouse monoclonal IgM	LY111	1:1000	Simona et al. 2017
anti-CS-C	Seikagaku	mouse monoclonal IgM	MC21	1:1000	Simona et al. 2018
anti-5-HT	ImmunoStar	rabbit polyclonal IgM	1394	1:100	Jung-Yu et al. 2006
anti-5-$HT_{2c/a}$	Abcam	rabbit polyclonal IgM	ab37293	1:100	Philippa et al. 2018
anti-5-HT_7	Abcam	rabbit polyclonal IgM	ab61563	1:200	
anti-RPTPσ	R&D systems	goat polyclonal IgM	AF3430	1:100	Mattias et al. 2020
anti-LAR	Abcam	goat polyclonal IgM	ab118456	1:100	
anti-C4ST-1	Invitrogen	rabbit polyclonal IgM	PA5-62697	1:200	

Figures

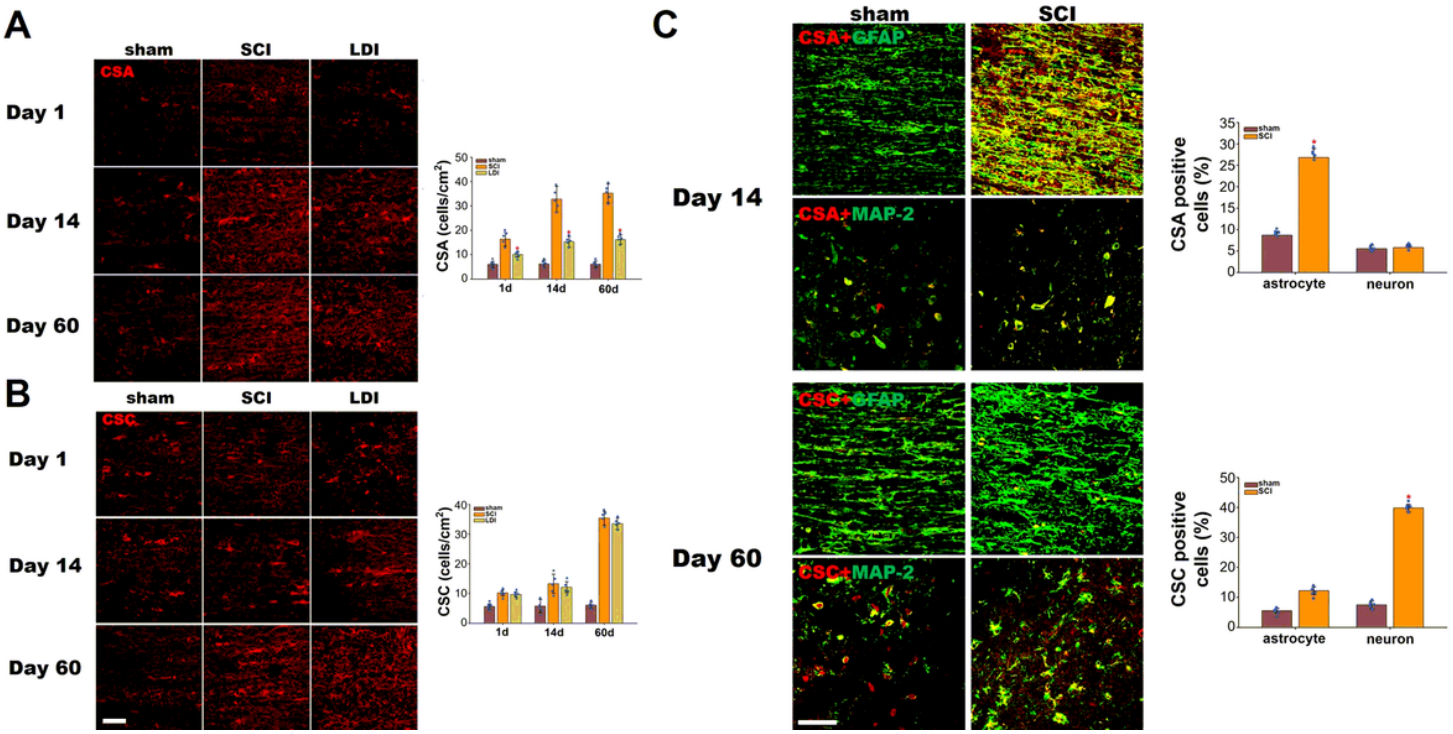

Figure 1

The temporal expression and cellular localization of CS-A and CS-C proximal to the lesion following SCI. (A) Immunofluorescent staining showing that CSA expression was induced after SCI(n=5) and was strongly attenuated by LDI (n=5) (*P < 0.05). (B) Although CS-C increased at 14-days post-SCI (n=5)and reached a peak at 60-days post-SCI, LDI treatment(n=5) showed no inhibitory effect on CS-C expression. Scale bar = 50 μm. (C) At 14-days post-SCI(n=5), colocalization of CS-A and GFAP was also apparent, but rare expression of CS-A was observed in MAP-2 positive neurons/axons. At 60-days post-SCI(n=5), CS-C was upregulated in both neuron/axons and astrocytes proximal to the lesion (*P < 0.05). Scale bar = 50 μm.

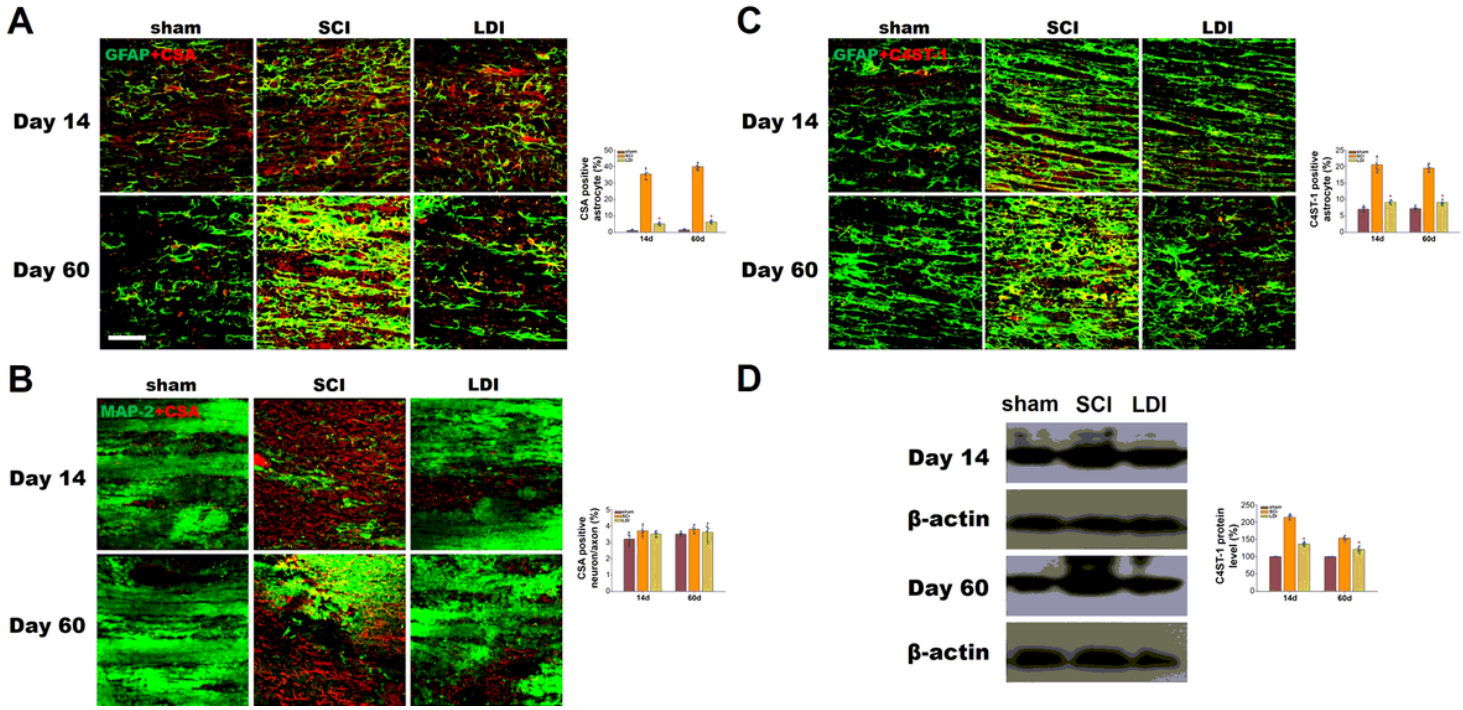

Figure 2

LDI decreases astrocyte-associated CS-A expression after SCI. (A) Representative GFAP (green)/CSA (red) double-staining images. Immunofluorescent staining showing that GFAP and CSA expression were induced after SCI(n=5) and were strongly attenuated by LDI(n=5) (*P < 0.05). Scale bar = 50 μm. (B) Representative MAP-2 (green)/CSA (red) double-staining images. Immunofluorescent staining showing that LDI(n=5) had no effect on neuron-associated CS-A expression (*P < 0.05). Scale bar = 50 μm. (C) Representative GFAP (green)/C4ST-1 (red) double-staining images. Immunofluorescent staining showing that LDI treatment (n=5)significantly inhibited C4ST-1 expression in astrocytes (*P < 0.05). Scale bar = 50 μm. (D) Immunoblotting results of C4ST-1 in sham-operated, SCI, and LDI groups at 14- and 60-days post-SCI (*P < 0.05).

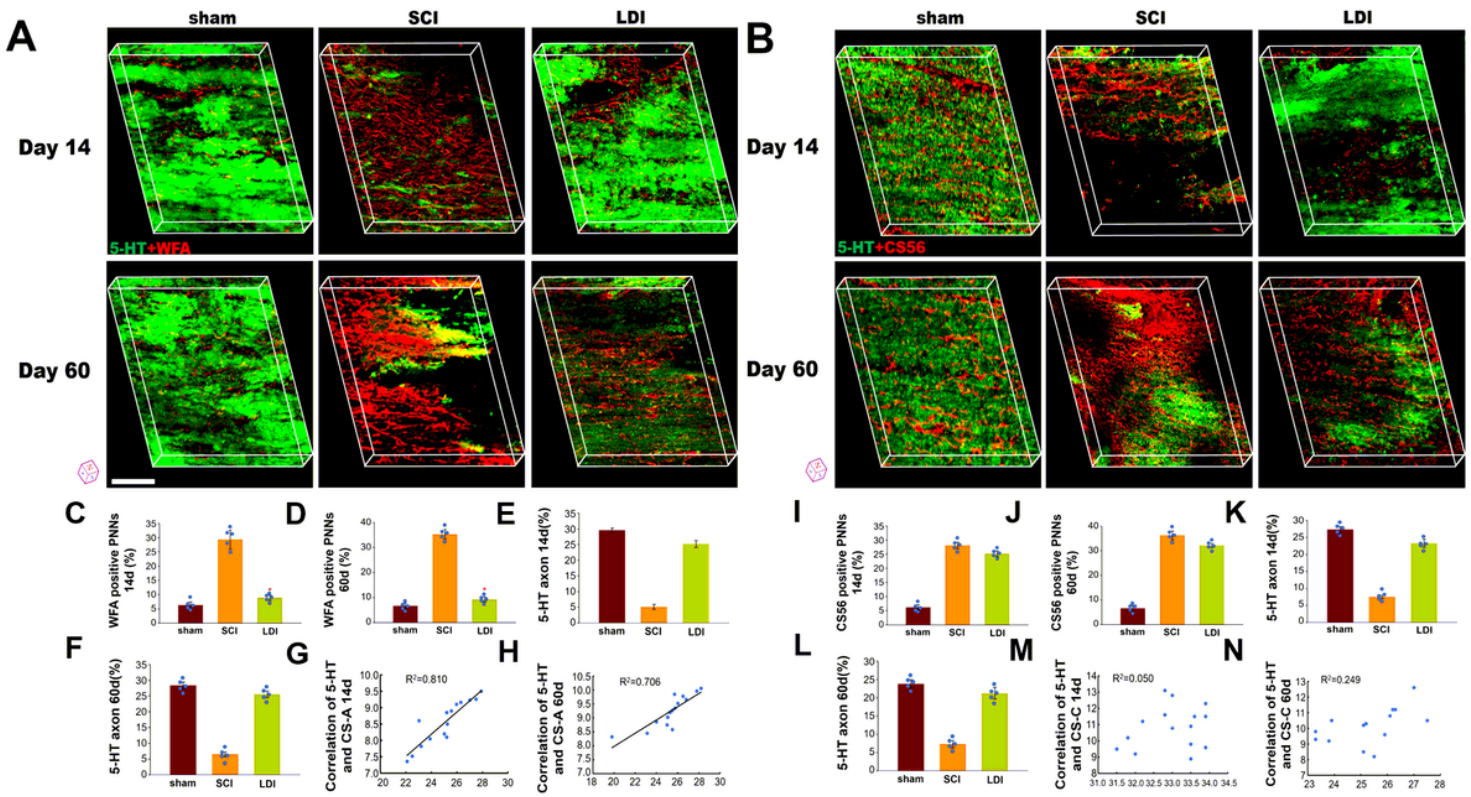

Figure 3

LDI promotes 5-HT axons expression accompanied with decrease of CS-A-enriched PNNs. In the SCI group(n=5), 5-HT axons were repelled in a comparable manner to CS-A-enriched PNNs (A) and CS-C-enriched PNNs (B) proximal to the lesion. LDI(n=5) significantly reversed CS-A-enriched PNN accumulation and and promoted 5-HT-positive axonal regeneration (*P < 0.05), but no inhibitory effect on CS-C-enriched PNN accumulation. Scale bar = 50 μm. (C-F) The percentage of WFA positive PNNs and 5-HT axon at 14-days and 60days post-SCI(n=5). (G,H) There was a significant correlation between a reduction of CS-A-enriched PNNs and an increase of 5-HT axonal immunoreactivity. (I-L) The percentage of CS56 positive PNNs and 5-HT axon at 14-days(n=5) and 60days(n=5) post-SCI. (M,N) There was no significant correlation between a reduction of CS-C-enriched PNNs and an increase of 5-HT axonal immunoreactivity.

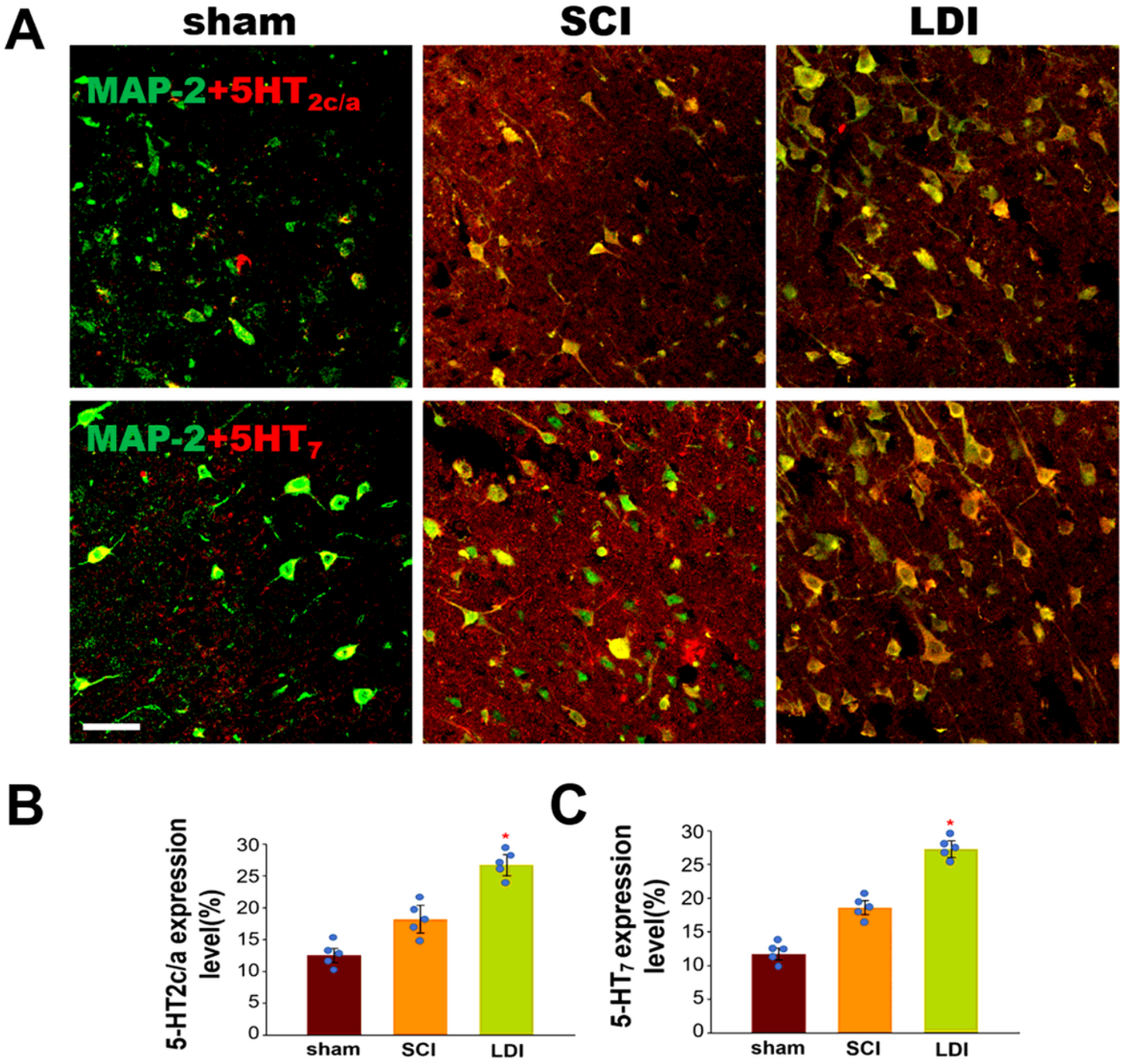

Figure 4

LDI increases 5-HT receptor expression after SCI. (A) Representative MAP-2 (green)/5-HT2c/a (red, A) and 5-HT7 (red, B) double-staining images. Immunofluorescent staining showed that LDI(n=5) increased 5-HT receptor expression in neurons. Scale bar = 50 μm. (B) The 5-HT2c/a expression levels in sham-operated(n=5), SCI(n=5) and LDI(n=5) groups (*P < 0.05). (C) The 5-HT7 expression levels in sham-operated(n=5), SCI(n=5) and LDI(n=5) group (*P < 0.05).

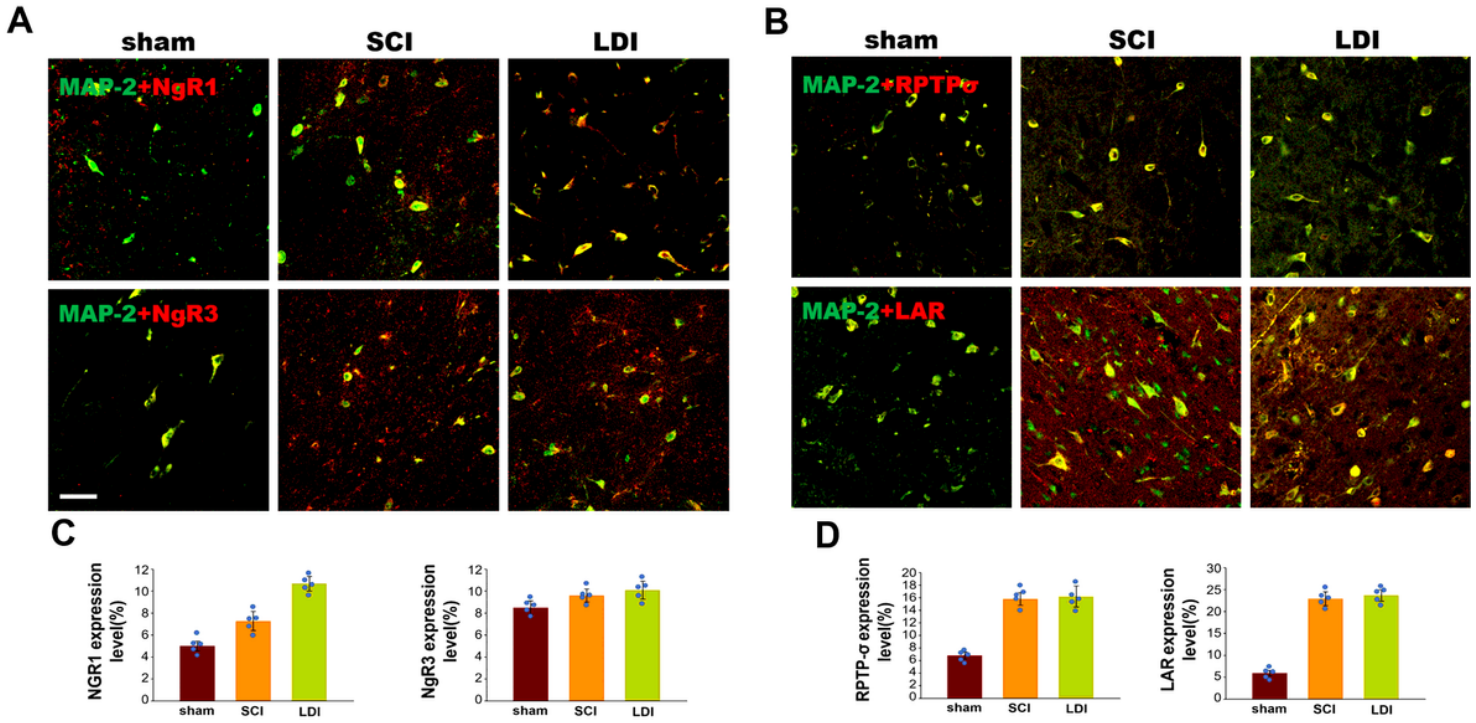

Figure 5

LDI has no effect on NgR, RPTPσ or LAR receptors after SCI. (A, C) Representative MAP-2 (green)/NgR (red) double-staining images. There was no significant difference in the expression of NgR1 or NgR3 between the SCI group(n=5) and LDI(n=5) group. Scale bar = 50 μm. (B, D) Representative MAP-2 (green)/RPTPσ and LAR receptor (red) double-staining images. There was no significant difference in the expression of RPTPσ or LAR between the SCI group(n=5) and LDI group(n=5). Scale bar = 50 μm.

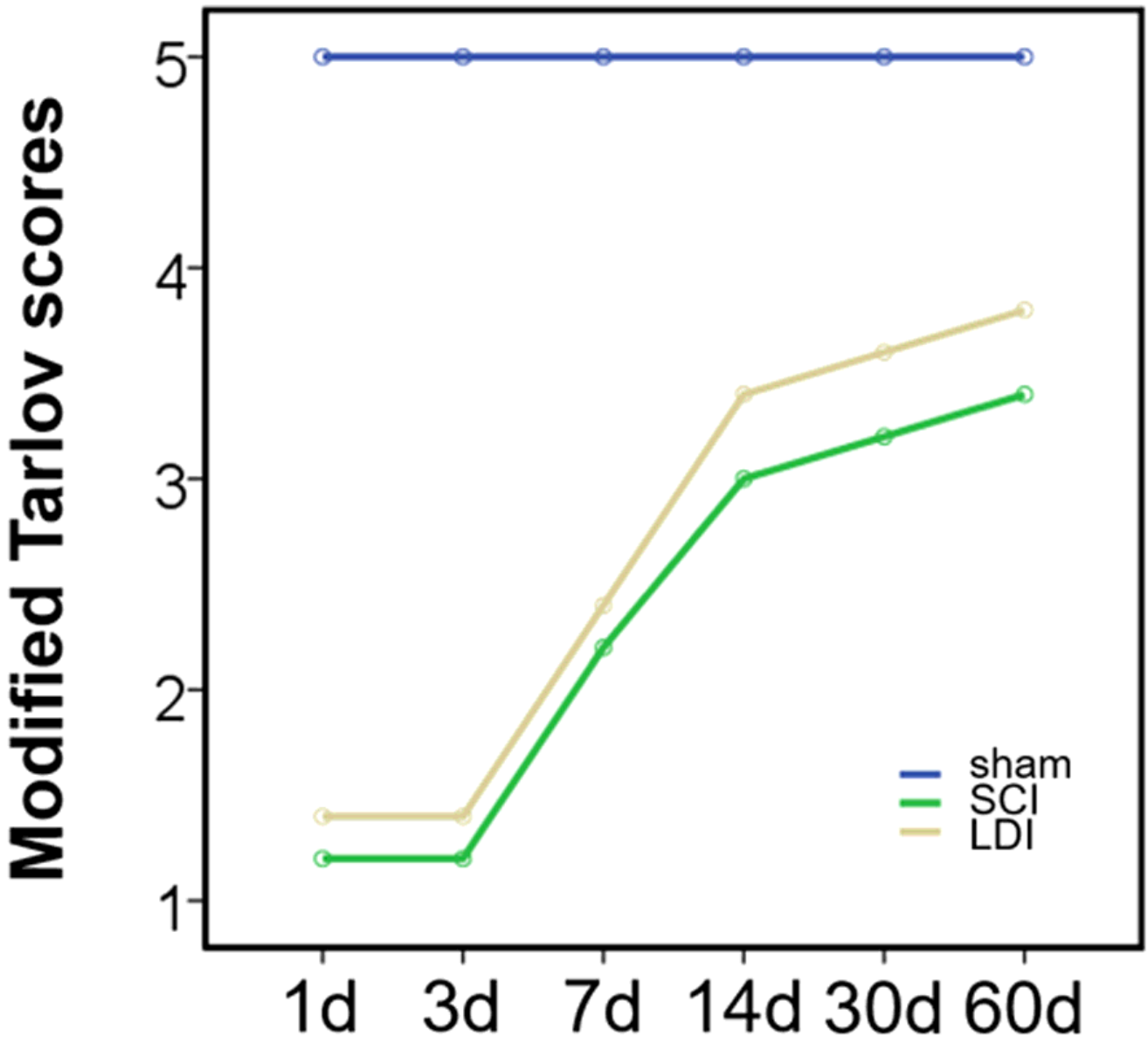

Figure 6

LDI promotes motor-function recovery after SCI. Enhanced motor recovery occurred in the LDI-treated animals compared with the SCI-treated animals. The modified-Tarlov scores of sham-operated (n = 5), SCI (n = 5), and LDI (n = 5) groups at 1-, 3-, 7-, 14-, 30- and 60-days post-SCI are shown (*P < 0.05).

Supplementary Files

This is a list of supplementary files associated with this preprint. Click to download.

- S1.normalityandvariancehomogeneity.docx

- S2.Fullwesternblotbandsfilm.pptx